Journal of Hydrology 568 (2019) 275–284

Contents lists available at ScienceDirect

Journal of Hydrology

journal homepage: www.elsevier.com/locate/jhydrol

Coastal wetland resilience to climate variability: A hydrologic perspective

Yu Zhang[a,*], Wenhong Li[a], Ge Sun[b], John S. King[c]

[a] Earth and Ocean Sciences, Nicholas School of the Environment, Duke University, Durham, NC 27708, USA
[b] Eastern Forest Environmental Threat Assessment Center, Southern Research Station, United States Department of Agriculture Forest Service, Raleigh, NC 27606, USA
[c] Department of Forestry and Environmental Resources, North Carolina State University, Raleigh, NC 27695, USA

ARTICLE INFO

Keywords:
Coastal wetland
Wetland resilience
Hydrologic model
Climate variability
Tipping point
Absorption and restoration

ABSTRACT

Climate-induced disturbances are expected to increase in frequency and intensity and affect wetland ecology by altering its hydrology. Investigating how wetland hydrology responds to climate disturbances is an important first step to understand the ecological response of coastal wetlands to these disturbances. Wetland hydrologic resilience, the ability of wetland in absorbing disturbances and restoring to pre-disturbance conditions in hydrological function, is a critical measure of wetland hydrological response to climate disturbances. However, a practical methodology for quantifying wetland hydrologic resilience (HR) is still lacking. This study aimed to improve the approach for quantifying the hydrologic resilience of wetland ecosystems to climate variability and climate change. A set of quantitative metrics was developed including the variations of groundwater table, overland flow, and saltwater table. This approach was then applied to a coastal landscape that includes coastal-forested and herbaceous wetlands in North Carolina, USA. We investigated the threshold behaviors of groundwater table, overland flow, and saltwater table for a 20-year period (1995–2014) by applying a regional scale wetland hydrological model, Penn State Integrated Hydrological Model for wetland hydrology (PIHM-Wetland). We found that the multiscale variations of groundwater table under dry climatic conditions is a good indicator of wetland HR to drought. The variation of overland flow during rainfall events effectively quantified HR to wet periods. We also found that the variation of the water level of saltwater is an important metric of wetland HR to sea level rise. This study improves the methodology of quantifying wetland hydrologic resilience at a regional scale, representing an important first step towards understanding the wetland hydrological and ecological resilience to future intensified climate disturbances in coastal regions and beyond.

1. Introduction

Climate change, comprised of rising temperature, changes in the intensity and frequency of rainfall, and accelerating sea level rise (SLR) over a wide range of temporal and spatial scales, is one of the most important threats to coastal wetland ecosystems (Burkett and Kusler, 2000; Mitsch et al., 2013). These climate-driven disturbances affect wetland ecological functions through altering wetland hydrological function, the capability of wetlands in storing and releasing water (Winter, 2000). For example, the decline of groundwater storage due to droughts may cause water stress on wetland vegetation (Rodríguez-Iturbe and Porporato, 2007) and enhance the emission of greenhouse gases (GHGs) from wetland soil (Burkett and Kusler, 2000). Flooding associated with storms and sea level rise may significantly increase soil erosion (Day et al., 2008) and the mortality of flood-intolerant vegetation (Conner et al., 2002). Furthermore, saltwater intrusion driven by the change in storage of freshwater and sea level rise may affect the survival and productivity of salt-intolerant plants (Williams et al., 2003). Thus, understanding how wetland hydrology responds to the changing climate is important for wetland ecosystem conservation.

Previous studies have focused on assessing and predicting the consequences of current and future climate disturbances on wetland hydrology (Desantis et al., 2007; Lu et al., 2009; Michener et al., 1997; Nicholls, 2004; Tufford, 2011; Zhu et al., 2017). However, most of these studies provided limited information about the threshold response of hydrological processes to climate disturbances. In other words, under what climate conditions/thresholds the wetland hydrological functions may be significantly altered are not clear. Such knowledge is urgently needed in wetland ecosystem management to respond to increasing climate change and sea level rise globally.

Wetland hydrologic resilience (HR) has been found as a useful concept to understand the threshold response of wetland hydrology to climatic disturbances (Peterson et al., 2012; Ridolfi et al., 2006). The term 'hydrologic resilience', which stems from the concept of

* Corresponding author.
E-mail address: yu.zhang4@duke.edu (Y. Zhang).

https://doi.org/10.1016/j.jhydrol.2018.10.048

Available online 27 October 2018

'ecological resilience', describes the ability of wetlands to absorb a disturbance and return to pre-disturbance hydrological function (Folke et al., 2002; Gunderson, 2000; Gunderson and Pritchard, 2012; Holling, 1973; Peterson et al., 2012). Following this concept, studies have quantified the hydrologic resilience of ecosystem from two aspects: (1) the "size" of disturbances that an ecosystem could withstand without changing its original hydrological function, and/or (2) the "return rate" to its prior hydrological states after disturbances (Gunderson, 2000). For example, Richter et al. (1996) developed a method for assessing the threshold of climate condition under which the hydrological processes were altered. They used monthly and yearly stream flow to quantify hydrologic alterations under human and climate disturbances. This method efficiently detected the change of hydrologic regimes associated with long-term disturbances (e.g., the dam effect and year-round groundwater pumping) (Richter et al., 1996). However, the method does not well capture the hydrological alteration under short-term disturbances (e.g., hurricanes, rainfall storms, and droughts). In vulnerable systems, a short-term climate disturbance may cause dramatic hydrological alteration with ecological and social consequences (Folke, 2006). Peterson et al. (2012) improved the representation of hydrological responses to shorter temporal scale disturbances by using an analytical resilience method. In their study, the dynamics of groundwater table (GWT) in a lumped artificial unconfined aquifer was used as a metric to quantify wetland resilience (Peterson et al., 2012). Two separate (deep and shallow) stable states of GWT were identified under constant annual precipitation with dry and wet initial conditions (Peterson et al., 2012). After identifying the stable states, Peterson et al. (2012) examined the deviation of GWT from the stable states under stochastic precipitation series with different annual intensity. They found that, with the increase in precipitation, GWT near the deep steady state is more resilient to large rainfall events than the GWT near the shallow stable state because the lower steady-state enabled large storage rooms for large rainfall, thus can absorb more rainfall. However, due to the non-linearity of wetland dynamics, the steady states of GWT under annual averaged rainfall may not represent the stable states of the water table at daily-, weekly-, and monthly-scales. Additionally, the ecosystem heterogeneity was not considered in the lumped modeling framework, which might cause large uncertainties in quantifying the hydrologic resilience of an actual ecosystem (Montefalcone et al., 2011). Furthermore, using only one hydrological variable (e.g., flow rate in Richter et al. (1996) and GWT in Peterson et al. (2012)) may not be sufficient to effectively reflect the hydrologic resilience of an ecosystem where a full hydrological cycle is involved.

To comprehensively quantify the hydrologic resilience of actual wetland ecosystems with high landscape heterogeneity, our study aimed to improve the methodology of quantifying wetland hydrological resilience of actual wetland ecosystems. We developed a set of comprehensive metrics (e.g., groundwater table, overland flow rate, and saltwater table) to enhance the state of knowledge on coastal wetland resilience at multi-spatial and temporal scales. The application of the approach to coastal forested and coastal herbaceous wetlands in North Carolina, USA, demonstrated the effectiveness of the proposed quantitative method for quantifying hydrologic resilience of coastal wetlands.

2. Methodology

2.1. Quantification of wetland hydrologic resilience (HR)

To characterize wetland hydrologic resilience, we focused on quantifying (1) the threshold intensity of climate disturbances that coastal wetland system could withstand without significant change in their hydrological function, and (2) the capability of recovering their hydrological function from disturbances to the pre-disturbance state. We defined "significant change in hydrological function" as the large deviation of the hydrological fluxes/states from their climatological mean. For example, we identified the change of the hydrological fluxes/states as statistically significant when the change was at least one standard deviation above or below the climatological mean.

The method proposed here emphasizes the hydrological interactions among upland, coastal-forested wetland, coastal herbaceous wetland, and the ocean, which together determine the hydrodynamics of coastal wetlands. We hypothesized that (1) due to the non-linearity of the complex wetland system, one or several thresholds of climate disturbances/forcing may exist, passing which the hydrological function may be significantly altered, and (2) the characteristics of ecosystem resilience may not be easily examined under a short time series analysis, thus a long time series analysis of the hydrological processes (e.g., decades) is needed.

We chose groundwater table (GWT), overland flow rate (OFR), and water table of saltwater (ST) as indicators of wetland hydrologic resilience (Level 1 in Fig. 1). The variations of these variables reflect the changes in wetland hydrological functions, in particular, the capability to store and release water. Wetland hydrology impacts wetland biogeochemical and morphological functions (Level 2 in Fig. 1) mainly through changing the GWT, OFR, and ST (the arrows linking Level 1 and Level 2 in Fig. 1) (Ardón et al., 2013; Cahoon et al., 2006; Desantis et al., 2007; Ferguson and Gleeson, 2012).

Since hydrologic resilience could present different features across scales (Gunderson and Pritchard, 2012; Montefalcone et al., 2011; Thrush et al., 2009), this method aims to study the variations of GWT, OFR, and ST on multiple spatial and temporal scales to reveal the nonlinearity of wetland ecosystems. Specifically, we first analyzed the climatic forcing and identified climate variability and extremes (e.g., dry and wet years, large rainfall events, and droughts). Then, we quantified the hydrologic resilience by examining the self-adaptive cycles of GWT, OFR, and ST at the seasonal and inter-annual scales. Next, we investigated the response of GWT, OFR, and ST to climate extreme events on the daily scale. Last, we quantified the spatial variation of hydrologic resilience to climate disturbances by examining the spatial variations of GWT, OFR, and ST under climate extreme events (Table 1).

2.2. Study area

The study area is the Albemarle-Pamlico peninsula on the lower coastal plain of eastern North Carolina with an area of 2784 km^2 (Fig. 2). The area experiences little disturbances from human activities. The elevation is higher at the west and lower at the east with an elevation relief of approximately 7 m (Fig. S1). The domain generally consists of forested wetland (78% of the study area) and emergent herbaceous wetland (3% of the study area) (Fig. 2). Vegetation height varies from 0.6 m for the herbaceous wetland to up to 20 m for the forest. Moorhead and Brinson (1995) derived the distribution of each wetland community type based on the National Wetlands Inventory (NWI). The majority of vegetation types in the forested wetland are an evergreen forest (50%) and a mixed forest (40%), and the majority of vegetation types in the emergent herbaceous wetland are marsh (60%) and shrub (40%) (Moorhead and Brinson, 1995). In terms of tolerance to salinity, the highly salt-tolerant vegetation, saltwater marsh, mainly occurs in the coastal zone within 200–300 m from the shoreline (Kemp et al., 2009). Although no studies have documented the detailed distribution of vegetation species in the forested wetlands, Richardson (1991) generally described that the forested wetland as consists of highly salt-tolerant trees (e.g., *Persea borbonia*), moderately salt-tolerant trees (e.g., *Magnolia virginiana*), moderately salt-tolerant shrub (e.g., *Ilex glabra*) and weakly salt-tolerant shrub (e.g., *Aronia arbutifolia*) (the level of salt-tolerance of these vegetation species refers to Graetz (1973)). A fully instrumented eddy flux observation tower is located in the Alligator River National Wildlife Refuge (red[1] star in Fig. 2) to

[1] For interpretation to colours in this fig. 2, the reader is referred to the web version of this paper.

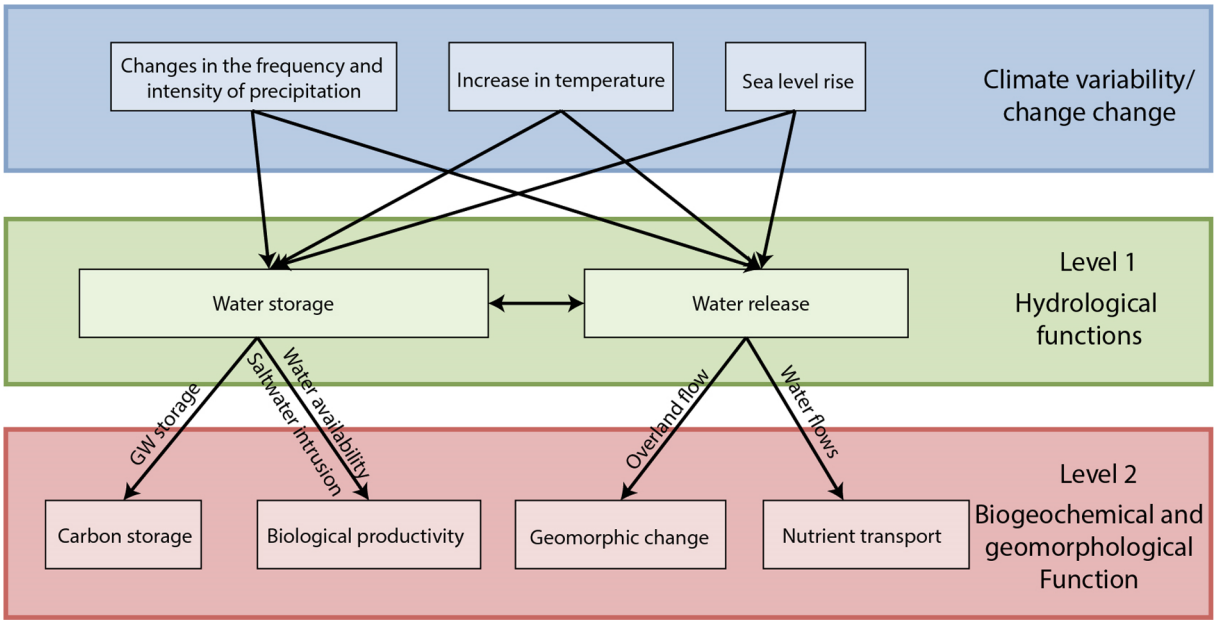

Fig. 1. Illustration of the influence of climate variability/change on the hydrological, biogeochemical, and geomorphological functions of coastal wetlands.

Table 1
Summary of hydrological variables used as indicators of hydrological resilience.

Hydrological variables	Wetland types	Climate disturbances and Scales	Measurable characteristics of resilience
Groundwater table (GWT)	Averaged value over forested and herbaceous wetland domain, respectively	Seasonal and inter-annual climate variability (precipitation, temperature, and sea level rise)	The capability of groundwater table in returning to a climatological mean groundwater table
	Averaged value over forested and herbaceous wetland domain, respectively	Duration of no rainfall at daily scale	Groundwater table drop rate
Overland flow rate (OFR)	Averaged value over forested and herbaceous wetland domain, respectively	Intensity of effective rainfall rate at daily scale	Increase rate of overland flow
	Spatially distributed value over forested and herbaceous wetland domain, together	Intensity of effective rainfall rate at daily scale	Spatial variation of overland flow rate
Saltwater table (ST)	Averaged value over saltwater intrusion region	Seasonal and inter-annual climate variability (precipitation, temperature, and sea level rise)	The variation of saltwater table at seasonal and inter-annual scales
	Averaged value over saltwater intrusion region	Extreme wet and dry climate condition	Spatial distribution of the difference between the highest and lowest saltwater table

measure energy fluxes, precipitation, temperature, humidity, carbon flux, soil respiration, groundwater table dynamics, and soil water content. Mean annual temperature of the study area is about 16.9 °C (1971–2000), with the lowest and highest temperature of 6.8 °C and 26.5 °C in January and July, respectively (Miao et al., 2013). According to local sea level observations, the mean sea level has increased by 0.083 m from 1995 to 2014 (NOAA, 2017). The soil is an organic muck (hydric soil water regime), underlain by poorly drained Pleistocene sedimentary deposits (Riggs et al., 1992). The groundwater table (GWT) of the forested wetland varied between 0.3 m below ground surface to 0.3 m above the ground surface from 2009 to 2011 (Miao et al., 2013). Our previous modeling study by Zhang et al. (2018) found that the averaged summer and winter GWT of the herbaceous wetland is about 0.1 m higher and 0.02 m lower than those in the forested wetland, respectively.

2.3. PIHM-Wetland model

To simulate surface and subsurface hydrological processes, we used PIHM-Wetland (a new version of Penn State Integrated Hydrological Model (PIHM) developed for wetland hydrology), a physically-based, distributed hydrologic model fully coupling coastal processes (e.g., tide, sea level rise, and saltwater intrusion) (Zhang et al., 2018). The model domain was decomposed into unstructured triangular mesh, and the hydrological processes were solved by using the semi-discrete finite volume method (Zhang et al., 2018). PIHM-Wetland tracks the changes of surface water, unsaturated and saturated soil water, saltwater, and canopy water by simulating water exchange through canopy interception, infiltration, overland flow, channel flow, unsaturated water flow, saturated water flow, saltwater lateral flow, and evapotranspiration. In PIHM-Wetland, the canopy interception is described as a function of leaf area index (LAI) (Dickinson, 1984; Kumar, 2009). If precipitation exceeds the capacity of canopy interception, precipitation drops to the land surface as throughfall. Overland flow and channel flow are represented by a two-dimensional simplified St. Venant Equation (Zhang et al., 2016), with a cell to cell routing processes. Overland flow occurs when precipitation rate exceeds infiltration rate (Infiltration excess overland flow) or soil is saturated (saturation excess overland flow). Soil water movement is described by a one-dimensional unsaturated flow and two-dimensional saturated flow, which are represented by Richard's equation and Darcy's saturated flow equation, respectively (Zhang et al., 2016). PIHM-Wetland assumes that fresh groundwater and saltwater form a clear freshwater-saltwater interface, and the saltwater lateral flow follows Darcy's law. The model also tracks water

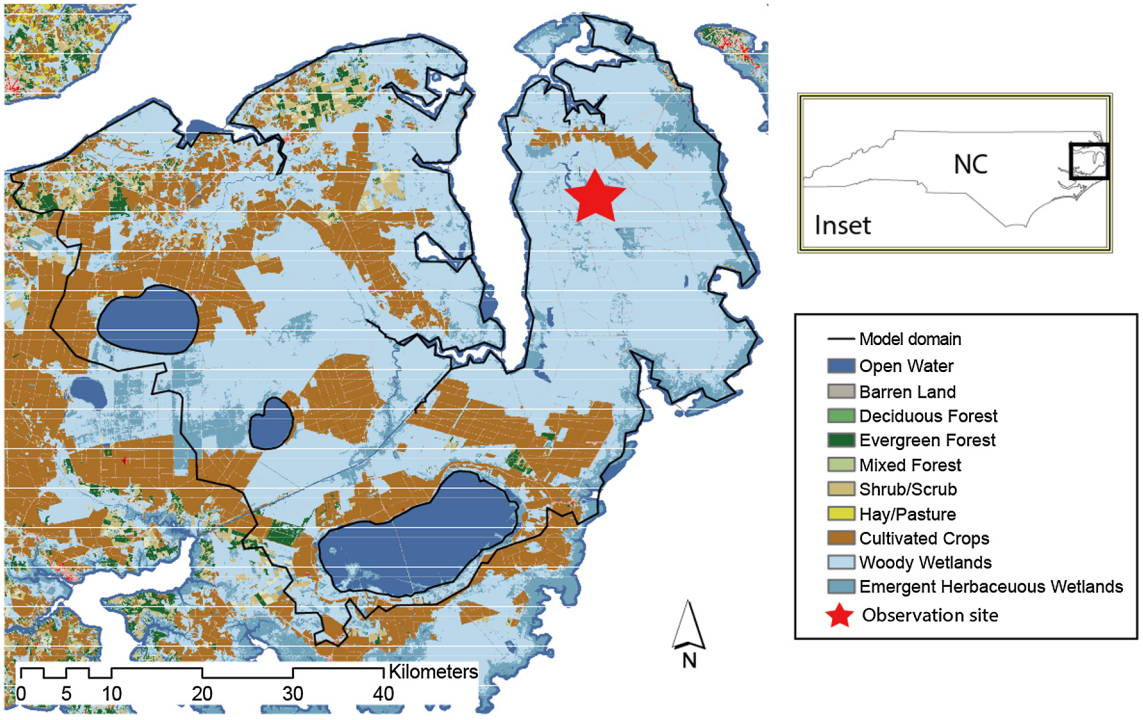

Fig. 2. The study area (35°24′48″N, 76°40′15″W - 36°5′11″N, 75°40′33″W) with land cover types. The red star indicates the observation site (35°46′34″N, 75°54′12″W). Inset: the location of the study area in North Carolina (NC). The black box in the inset indicates the study area. (For interpretation of the references to color in this figure legend, the reader is referred to the web version of this article.)

loss from soil evaporation, plant transpiration, and canopy evaporation, which are governed by the Penman-Monteith equation (Zhang et al., 2016). PIHM-Wetland is useful for the current study because (1) it has the ability to simulate regional-scale hydrological processes across environmental gradients, (2) it is physically-based and fully couples coastal processes, and 3) it is well-calibrated and validated for this site (Zhang et al., 2018). Details of the hydrological components of the model are referred to the literature (Kumar, 2009; Zhang et al., 2018; Zhang et al., 2016).

2.4. Data

PIHM-Wetland used the national dataset for meteorological forcing and parameterizations of soil and land cover properties. We used the time series of meteorological data from Phase 2 of the National Land Data Assimilation System (NLDAS-2) (Xia et al., 2012) as our forcing data, including precipitation, surface air temperature, specific humidity, air pressure, and solar radiation. NLDAS-2 has a spatial resolution of 0.125° and temporal scale of one hour (Xia et al., 2012). The adequacy of using the national meteorological dataset to the study domain is evaluated by Zhang et al. (2018), who found that the 20-year NLDAS-2 dataset agrees well with the observed meteorological variables from the observation sites. In the seasonal analysis, we defined the four seasons as spring (March-May), summer (June-August), fall (September-November) and winter (December of the current year and January and February of the following year).

The soil parameters, governing the processes of infiltration, recharge, and lateral groundwater flow, include vertical and horizontal hydraulic conductivity, porosity, and coefficients for the soil-water retention curve. These parameters were derived from the national Gridded Soil Survey Geographic (gSSURGO) database that provides soil texture, organic matter content, and soil bulk density at different depths of soil layer (Soil Survey Staff, 2016). The derivation of the soil parameters can be found at Wösten et al. (1999). The gSSURGO dataset shows that the well-drained soil is mainly located at the top 0–0.3 m soil zone where the soil is rich in coarse organic matter, and the bottom soil layer (below 0.3 m) is poorly drained substrate, which is consistent with the field measurement studies (Bruland and Richardson, 2006; Moorhead and Brinson, 1995). The dataset also has a good spatial representation of soil type variability because of its fine spatial resolution (30 m) (Soil Survey Staff, 2016). The soil map can be found in the supplementary information (Fig. S2).

The land cover parameters, governing the processes of evapotranspiration, overland flow, and energy budget, are maximum leaf area index (LAI), minimum stomatal resistance, reference stomatal resistance, albedo, vegetation fraction, Manning's roughness, and root zone depth. These parameters were obtained from the National Land Cover Dataset (NLCD) (Fry et al., 2011) and the Monthly Vegetation Database (https://ldas.gsfc.nasa.gov/nldas/web/web.veg.monthly.table.html) that is widely used in the land surface models, such as BAT (Dickinson et al., 1993), Sib (Sellers et al., 1986), CLM (Dai et al., 2003), and Noah LSM (Chen et al., 1996). Based on the NLCD land cover classification in 2011, there are 10 land cover types in the study domain, including open water, barren land, deciduous forest, evergreen forest, mixed forest, shrub/scrub, herbaceous, cultivated crops, woody wetlands, and emergent herb wetlands (Fig. 2).

For the coastal processes, we obtained the tidal observations from the Oregon Inlet Marina station (Station ID: 8652587) of NOAA (National Oceanic and Atmospheric Association) Tide and Current (https://tidesandcurrents.noaa.gov/). The absolute height of hourly tide was calculated by adding the relative tide height above mean sea level (MSL) to the MSL. According to the mean sea level trend in NOAA, we used a linear function, $MSL = \frac{0.0003t}{43200} + 0.019$, to represent sea level rise, where t is the time from 1995 to 2014 (unit: minute, and $t = 0$ on Jan 1st, 1995).

2.5. Model setup

We conducted a 20-year hydrological simulation from 1995 to 2014 with the one-minute time interval for simulation and the daily time step

for outputs. The study domain was decomposed into 6290 unstructured triangular elements with the closed boundary condition, except the open boundary condition near the coastline, where the coastal processes interact with the hydrological processes on land (Fig. S3). The average size (longest edge) of the elements was around 100 m with finer elements located at the areas with a higher heterogeneity of land cover, topography, and soil. According to the soil features from the gSSURGO dataset and in situ measurements, the model set two soil layers, comprised of a well-drained top layer (0–0.3 m) and poorly drained bottom layer (0.3–1 m), by assuming that the subsurface hydrological activities primarily occur in the top one-meter soil zone. We set the initial GWT to be 0.1 m below ground surface with no surface water for the model domain. The lake level was set to be constant through time. The model simulation started after a five-year spin-up run, by which the system reaches a relative equilibrium state. The model parameters are summarized in Tables S1 and S2.

3. Results

3.1. Long-term climate variability/change

Precipitation and temperature data from the NLDAS-2 product and in-situ measurements from the observation site (red star in Fig. 2) were used to analyze the impact of climate on wetland hydrology during 1995–2014. Validation of the NLDAS-2 products indicated that the NLDAS-2 data reasonably captured the meteorological conditions in this area (Zhang et al., 2018). The 20-year averaged annual precipitation was 3.4 ± 0.4 mm/day, and the annual air temperature was 18.3 ± 2 °C. The seasonal and inter-annual variations of precipitation were larger than the seasonal and inter-annual variations of temperature from 1995 to 2014 (Fig. 3a and b). Storms and hurricanes contributed significantly to high rainfall in summer (Miao et al., 2013). To better understand hydrological responses to climate variability and climate change, we classified the 20-yr period into dry years, wet years, and normal years based on annual precipitation. There were three dry years (1997, 2001, and 2007) (colored in orange in Fig. 3) and three wet years (1996, 2003, and 2009) (colored in light blue in Fig. 3), where the annual precipitation anomaly is lower and higher than one standard deviation of the climatological mean precipitation, i.e., 0.42 mm/day, respectively, following Li et al. (2011). The remaining 14 years were normal years (colored in gray in Fig. 3). In general, precipitation in all seasons during the wet years was higher than that in the dry years (Fig. 3a). For example, in 2003 (a wet year), the annual mean precipitation was two standard deviations above the 20-year climatological mean. Similarly, the annual mean precipitation of 2001, a dry year, was 33% lower than two standard deviations below the 20-year climatology.

In order to understand the hydrological response to climate extremes, we defined heavy-rainfall events with their daily precipitation rates higher than the 75th percentile of the precipitation distribution, equivalent to 13 mm/day (See the precipitation distribution in Fig. S4). In contrast to precipitation, the magnitude and variation of annual mean temperature are about the same during dry and wet years (Fig. 3b).

According to NOAA tide and sea level observation near the coast of the study area, the sea level presents clear seasonal and inter-annual variations during the 20-yr period (Fig. 3c). Seasonal sea level varied within 0.05 m each year. The annual sea level first decreased from 1996 to 2002 followed by a gradual increase from 2003 to 2006. Annual sea level dropped in 2007, after which it increased again from 2008 to 2014. The overall sea level increased about 0.08 m from 0.019 m in 1995 to 0.099 m in 2014.

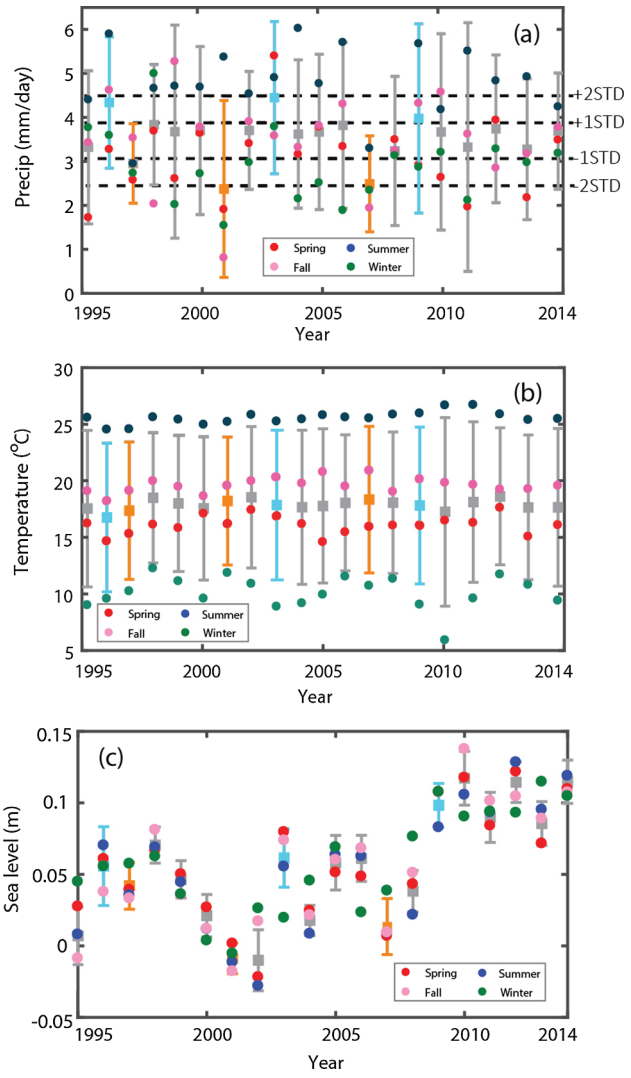

Fig. 3. Variation in domain averaged (a) precipitation (mm/day), (b) surface air temperature (°C), and (c) sea level (m) during 1985–2014. Grey squares and colored dots represent the annual and seasonal mean, respectively. The dashed black lines in (a) indicate one and two standard deviations (STD) above and below the 30-year climatological precipitation, separately. The dry and wet years are plotted in orange and light blue bars, respectively. 1997, 2001, and 2007 are classified as dry years. 1996, 2003, and 2009 are wet years. (For interpretation of the references to color in this figure legend, the reader is referred to the web version of this article.)

3.2. Response of groundwater table to multi-scale climate disturbances

3.2.1. Seasonal and inter-annual groundwater table variations

The first component of the hydrologic metrics for quantifying the threshold response of wetland hydrology to climate variability is groundwater table (GWT). We first examined the spatial averaged seasonal and annual variations of GWT from the model simulation for the coastal-forested wetland (Fig. 4a) and the coastal herbaceous wetland (Fig. 4b), respectively. At the inter-annual scale, the GWT varied between 0.02 and 0.13 m below the ground surface for the coastal-forested wetland (middle point of the black bars in Fig. 4a) and between 0.025 and 0.1 m below the ground surface for the coastal herbaceous wetland (middle point of the black bars in Fig. 4b). The interannual variation of GWT was highly correlated with annual precipitation. The correlation coefficient between the two is 0.95 and 0.91 for the coastal-forested and coastal herbaceous wetland, respectively (both significant at 0.01 level). The annual mean GWT of the coastal herbaceous wetland

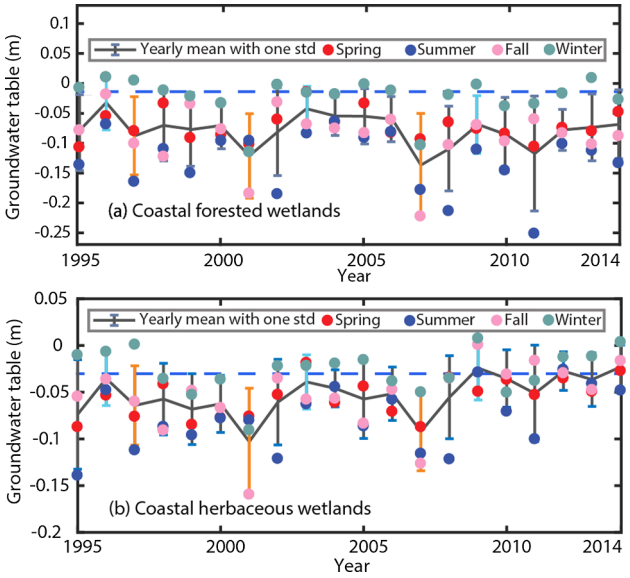

Fig. 4. Seasonal and annual mean GWT (unit: m) of (a) coastal forested wetland and (b) coastal herbaceous wetlands during 1995–2014. The black lines indicate the annual mean GWT with one standard deviation. Colored dots indicate the seasonal GWTs at each year. The blue dashed lines indicates the climatological mean of winter GWT. Annual GWT during the dry and wet years are plotted in orange and light blue bars, respectively. 1997, 2001, and 2007 are classified as dry years. 1996, 2003, and 2009 are wet years. (For interpretation of the references to color in this figure legend, the reader is referred to the web version of this article.)

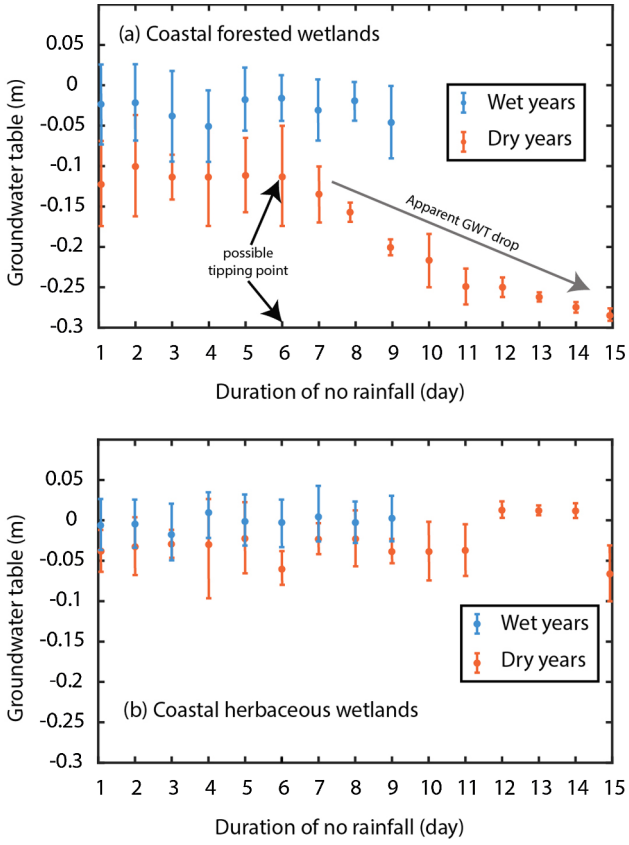

Fig. 5. The mean GWT (m) under the different duration of no rainfall for (a) coastal-forested wetland and (b) coastal herbaceous wetland, respectively. Each bar represents the averaged GWT under drought events with the same duration. The dots in the middle of the bars indicate the mean GWT, and the ends of the bars represent one standard deviation from the mean GWT.

showed a slight increase from 1995 to 2014 (Fig. 4b), which may be attributed to the increase in sea level during the period (Fig. 3c). However, no significant change of annual-mean GWT for the coastal-forested wetland was found, indicating that the influence of current sea level rise on GWT of the coastal-forested wetland was minor over the study period.

At the seasonal scale, GWT fluctuated widely, with a high GWT in winter and low GWT in summer in general. For the coastal-forested wetland, the winter GWT tended to return to its climatological winter GWT (−0.015 m) (blue dashed line in Fig. 4a) during 1995–2014, except the extremely dry years when the annual precipitation was two standard deviations lower than the climatological mean precipitation. Specifically, in the extremely dry years (i.e., 2001 and 2007), the winter GWT (−0.11 m and −0.3 m for 2001 and 2007, respectively) did not return to the climatological mean level. For the coastal herbaceous wetland, the seasonal variations of GWT were impacted by both precipitation and sea level variations. The winter GWT showed a larger seasonal variation compared to that of the coastal-forested wetland due to the regulation of sea level. Further, seasonal mean GWT in the extremely dry years (2001 and 2007) were apparently lower than that in the other years (Fig. 3a and b).

3.2.2. Daily scale groundwater table variation under climatic dryness

The GWT variations at the seasonal and annual time scales may dampen how GWT responds to climate events at finer time scales. Therefore, we analyzed the GWT variation under the different duration of no-rainfall on daily time scales. Fig. 5 shows the lowest daily GWT during different durations of no-rainfall in the dry (orange bars) and wet years (light blue bars) for the coastal-forested wetland (Fig. 5a) and coastal herbaceous wetland (Fig. 5b), respectively. Each bar represents the mean (middle dot) and one standard deviation (ends of the bar) of GWT during different drought events with the same duration. The longest duration of no rainfall was 15 days and 9 days during the dry and wet years, respectively. For the coastal-forested wetland, the GWT remained at a similar level in the wet years (about −0.02 m, Fig. 5a) even when drought reached its longest duration (nine days). The water level was approximately 0.1 m higher than that in the dry years (Fig. 5a). Likewise, the GWT (about −0.12 m) did not change much in the dry years when the no-rainfall days were shorter than six days. The stable groundwater level may be attributed to the stable hydrologic connectivity between aquifers because the water loss in the forested wetland can be easily compensated by water supplies from the upland and the coastal herbaceous wetland. However, when the drought duration was longer than six days in the dry years (Fig. 5a), the GWT dropped significantly with an increase in drought duration, because the hydrologic connectivity between aquifers weakened. The water supply from the upland and the coastal herbaceous wetland could not compensate for the water loss during long dry periods. The GWT declined approximately linearly when the dry periods exceeded 6 days (dashed line in Fig. 5a), with an averaged drop rate of 0.03 m per day. For the herbaceous wetland, the GWT remained at the similar level regardless of the dry and wet climate conditions mainly because of strong regulation by sea level (Fig. 5b).

3.3. Response of overland flow to multi-scale climate disturbances

3.3.1. The variation of overland flow under rainfall events

The second component in the metrics for quantifying the threshold response of wetland hydrology to climate variability is overland flow. Substantial studies have shown that overland flow responds quickly to rainfall events (Beven, 2011; Freeze, 1980; Lyne and Hollick, 1979). Thus, we focused on the threshold response of overland flow to individual rainfall events on daily scales; and the seasonal and inter-annual variations of overland flow can be found in Fig. S5. Fig. 6 shows

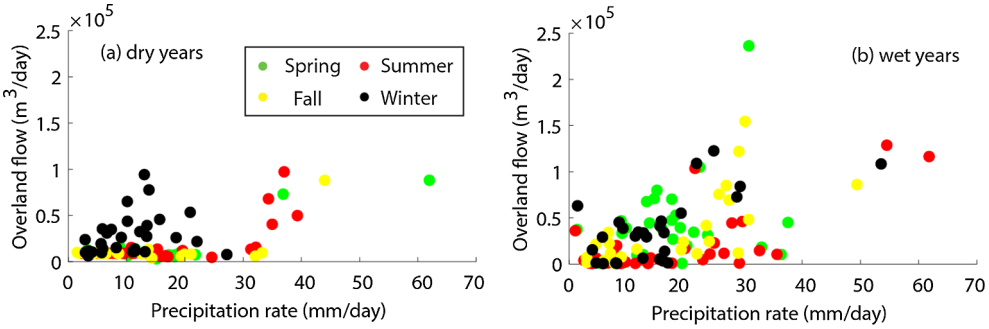

Fig. 6. Daily overland flow (unit: m^3/day) associated with different precipitation intensities (unit: mm/day) during (a) dry years and (b) wet years. Dots of different color indicate seasonal overland flow rates. (For interpretation of the references to color in this figure legend, the reader is referred to the web version of this article.)

the relationship between daily overland flow and precipitation intensity in different seasons in the dry and wet years. In the dry years (Fig. 6b), large overland flow rarely occurred, especially in the spring, summer, and fall seasons when rainfall was less than 30 mm/day. This is because the relatively low soil water content during dry years provided sufficient water storage room for water infiltration and storage. The relatively large overland flow was observed in winter (black dots in Fig. 6a) because the soil was close to saturation due to shallow GWT in winter and provided a limited capacity for water infiltration and storage. However, during the wet years, overland flow rates were approximately two to ten times greater than those during the dry years, and the high flow rate occurred in all seasons (Fig. 6b) because soil saturation level was high throughout the year, making the overland flow more likely to occur in the wet years.

3.3.2. Spatial variation of overland flow during large rainfall events

Our previous work demonstrates that the hydrological processes of coastal wetland respond differently to seasonal climate variability across environmental gradient (Zhang et al., 2018). We, therefore, examined the spatial variation of the overland flow rate under large rainfall events. To better understand the magnitude and distribution of overland flow rate, we also analyzed the spatial distribution of subsurface flow rate during large rainfall events. Fig. 7 shows the maximum rates of surface and subsurface water passing through the edges of each triangular element at different elevations in the decomposed model domain. Each dot represents the water flow rate on each cell with different elevation during each individual rainfall event. We focused on the spatial variation of water flow under rainfall events higher than 13 mm/day (> 75th percentile of the rainfall distribution in Fig. S4), upon which soil erosion is more likely to happen.

For overland flow distribution (Fig. 7a), the elements with high flow rate were located in the region with elevation between -0.5 m and 2 m (light green shaded area in Fig. 7a), especially the extremely high flow region with elevation between 0.2 m and 0.7 m (light orange shaded area in Fig. 7a). The overland flow rate was relatively low at the regions with the elevation higher than approximately two meters. It is estimated that, spatially, the regions with high and extremely high overland flows occupied 82% (light green in Fig. 7b) and 39% (orange in Fig. 7b), respectively, of the study domain when daily precipitation was higher than 13 mm/day. In contrast, the subsurface flow rate was much lower than overland flow rate during large rainfall events (> 13 mm/day) because a large proportion of the rainfall becomes overland flow without infiltrating to the soil zone (e.g., infiltration excess runoff generation). The elements with relatively high subsurface flow rate were located in a much narrower region with elevation between 0.4 m and 0.6 m (light blue shaded area in Fig. 7c) occupying 25% of the study domain (light blue in Fig. 7d), beyond which the subsurface flow rates were small regardless of the intensity of rainfall.

3.4. Response of saltwater intrusion to multi-scale climate disturbances

3.4.1. Seasonal and inter-annual variations of saltwater table

The third metric for quantifying the threshold response of wetland hydrology to climate variability is saltwater table. Saltwater intrudes

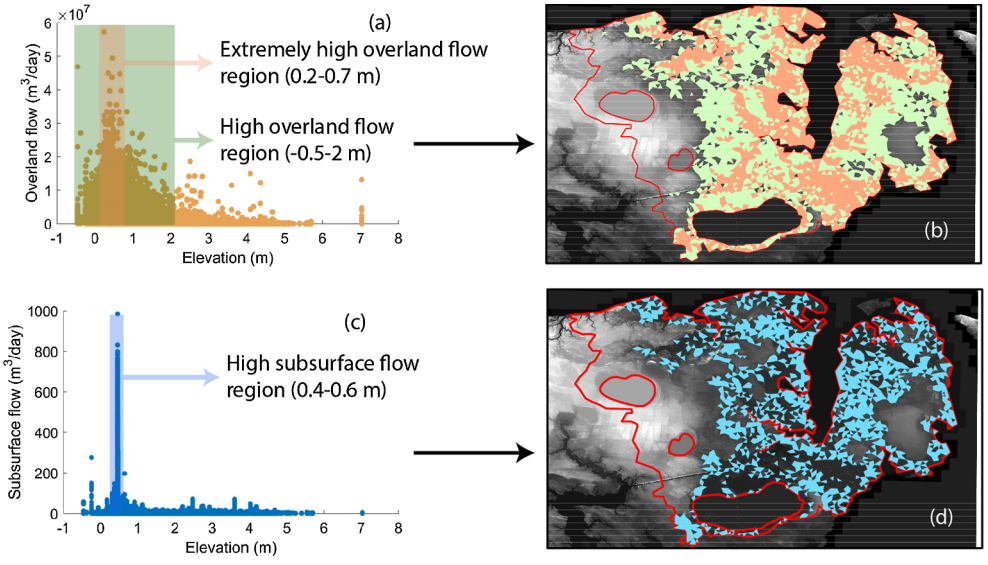

Fig. 7. Distribution of overland and subsurface flow rates (unit: m^3/day) during large rainfall events (higher than the 75th percentile of the 30 years' rainfall distribution) from 1995 to 2014. (a) Overland flow rate on each model cell at different elevations. Each dot represents each model cell. Green and orange shaded zones indicate the cells with high and extremely high overland flows, respectively. (b) Geographic distribution of the cells with high and extremely high overland flows. The green and orange cells are corresponding to the cells in the green and orange zones in (a). The gray background is the elevation map with higher elevation in white and low elevation in black. The red line denotes the model boundary. (c) is the same as (a) but for subsurface flow. The light blue shaded zone highlights the cells with the high subsurface flow. (d) is the same as (b) but for subsurface flow. The light blue cells are corresponding to the cells in the light blue zone in (c). (For interpretation of the references to color in this figure legend, the reader is referred to the web version of this article.)

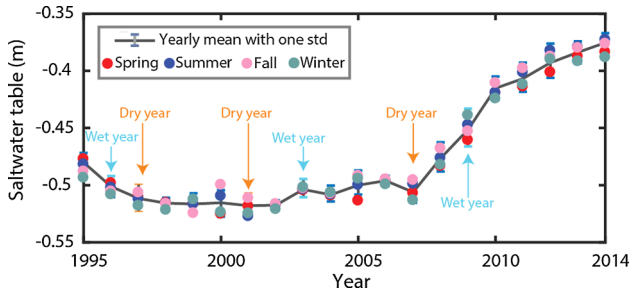

Fig. 8. Seasonal and inter-annual mean saltwater table (ST) (m) from 1995 to 2014. The black lines indicate the annual mean ST with one standard deviation. Colored dots indicate the seasonal ST at each year. Annual ST during the dry and wet years are plotted in orange and light blue bars, respectively, and are also indicated by the orange and light blue arrows. 1997, 2001, and 2007 are classified as dry years. 1996, 2003, and 2009 are wet years. (For interpretation of the references to color in this figure legend, the reader is referred to the web version of this article.)

into the coastal wetland due to the hydraulic head gradient between seawater and fresh groundwater (Fig. 8). Due to the higher density, intruded saltwater usually exists beneath fresh groundwater forming a saltwater-freshwater interface (Gupta, 1985; McElwee, 1985; Polo and Ramis, 1983; Shamir and Dagan, 1971). Seasonally, the saltwater table variation was small (within 0.025 m) even in the dry and wet years (see the colored dots in Fig. 8). Inter-annually, saltwater table (the black solid line in Fig. 8) is relatively smooth and flat from 1995 to 2007, after which saltwater table was apparently elevated from 2008 to 2014. Statistically, in general, the annual saltwater table variation was well correlated with the annual sea level variation (correlation coefficient of 0.72 at 95% confidence level), while the influences of annual precipitation and temperature on the saltwater table were secondary (correlation coefficient of 0.36 and 0.21 for precipitation and temperature at 95% confidence level, respectively).

3.4.2. Spatial distribution of saltwater table during extremely wet and dry periods

Although the influences of precipitation and temperature on the domain-averaged saltwater variation were secondary, it is interesting to know the spatial variation of the saltwater table under extremely wet and dry periods during the 20-year period. The extremely wet and dry periods are equivalent to the periods with the highest and lowest GWT, which were identified in December of 2009 (one of the wet years) and December of 2007 (one of the dry years), respectively. Fig. 9 shows the difference in saltwater depth between these two periods. The regions in dark blue and light colors represent the area without and with saltwater intrusion, respectively. The region with saltwater intrusion was mainly located in the low lying area near the coast (Fig. 9). The largest difference of saltwater depth in the extremely wet and dry periods was approximately 0.5 m, and the regions with the largest difference of saltwater depth were located hundreds of meters away from the coastline (yellow circles in Fig. 9). Notably, these regions indicate the critical region where freshwater processes strongly interact with the coastal processes. Towards the ocean, the interaction weakens, and the coastal processes dominate the dynamics of wetland hydrology. Towards the inland, the interaction weakens as well, and the freshwater processes dominate the hydrodynamics of the wetland.

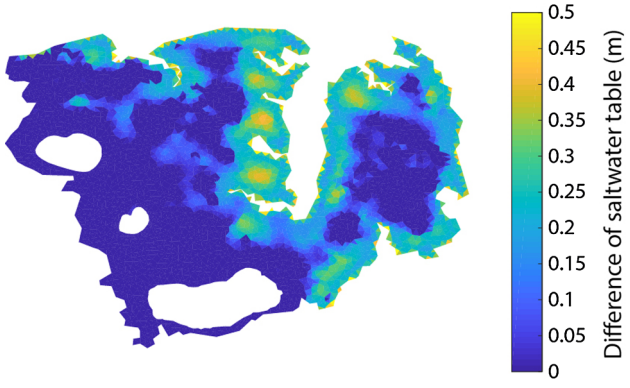

Fig. 9. Spatial distribution of the difference of saltwater table (ST) under extremely wet and dry periods. Color map represents the magnitude of the difference from low (dark blue) to high difference (yellow). The positive value on the color bar means that the ST in the extremely wet period is higher than that in the extremely dry period. (For interpretation of the references to color in this figure legend, the reader is referred to the web version of this article.)

4. Discussion

4.1. Hydrologic resilience of the coastal wetland

4.1.1. Hydrologic resilience to drought

At the seasonal and inter-annual scales, the GWT of forested wetlands in winter returned to the climatological mean, except during the extremely dry years when annual mean precipitation was two standard deviation below the 20-year climatological mean precipitation (Fig. 4a). This reveals the capacity of the coastal wetland to restore the GWT from dry climate conditions (less or no rainfall). Thus, seasonal and inter-annual variations of GWT can be used as an indicator of hydrologic resilience to dry climate conditions. This GWT-climate relationship reveals the hydrological adaptive cycle of the coastal wetland system (Holling and Gunderson, 2002). Large disturbances, like the extremely dry year, may delay and change the time and trajectory of the cycle.

We also found that GWT of forested wetland declined dramatically when the drought duration was longer than six days in the dry years (orange bars in Fig. 5a), indicating low resilience to drought under these conditions (Fig. 5a). On the other hand, the coastal herbaceous wetland was resilient to drought because the GWT level always stayed at a similar level (-0.04 m) even when the duration of drought reached its longest duration (blue and orange bars in Fig. 5b). Therefore, for forested wetlands, it appears a dramatic decline in hydrologic function may occur when the duration of drought exceeds the threshold of six days. This water stress condition may, therefore, have a large impact on the stability of other wetland ecological functions (Folke et al., 2004).

4.1.2. Hydrologic resilience to rainfall events

The event-based analysis found that overland flows were largely attenuated or prevented in the spring, summer, and fall during the dry years when the rainfall rate was less than 30 mm/day (Fig. 6), indicating hydrologic resilience to rainfall events of this magnitude during the dry years. However, in the wet years, the ecosystem became less resilient to rainfall because a small amount of rainfall caused large overland flow due to limited water storage capacity (Fig. 6b). The spatial distribution of overland flow suggests that high overland flow would occur on over 82% of the coastal wetland domain under heavy rainfall ($>$ 13 mm/day) (Fig. 7a and b), which reveals that the majority of the wetland is less resilient to heavy rainfall. Thus, understanding the threshold response of overland flow to rainfall events is important for predicting changes in wetland structure and function under heavy rainfall events. For example, a large overland flow may significantly increase land surface erosion and massive losses of biomass (Kirwan and Megonigal, 2013; Kozlowski, 2002), thereby changing the wetland morphological function. Additionally, flood frequency and duration can be critical for vegetation development through impacting on soil oxygen availability for root aerobic respiration, seed germination, and vegetation growth (Fagherazzi et al., 2004). Thus, the increase in flooding would accelerate the mortality of flooding intolerant plants (Conner et al., 2002).

4.1.3. Hydrologic resilience to sea level rise

Seasonally, the variation of the domain-averaged saltwater table was within 0.025 m (Fig. 8), which could be attributed to the slow response of saltwater diffusion to seasonal climate variability. In other words, the saltwater table variation is not sensitive to seasonal climate fluctuations, revealing that the wetland system could effectively absorb seasonal climate disturbance and retain its pre-disturbance saltwater table levels. Annually, the saltwater table was relatively flat with very few oscillations between 1995 and 2007 and increased obviously after 2007 (Fig. 8). Before 2007, the sea level control on the saltwater table was not apparent, although sea level presented 0.1 m annual variation. The relatively low sea level (averaged sea level of 0.04 m in Fig. 3c) would be the main reason for the relatively flat saltwater table profile. The wetland system could absorb the influence of the annual sea level change on the saltwater table variation. However, after 2007, the saltwater table increased apparently with the rise in sea level (averaged sea level of 0.1 m in Fig. 3c). The relatively high sea level presented dominant control on saltwater table variation. This suggests that the sea level of 0.1 m after 2007 would be equal to or higher than the sea level threshold, above which the wetland system cannot absorb the influence of sea level rise on saltwater table variation. Spatially, the largest difference of saltwater table between the extremely dry and wet periods was up to 0.5 m (the areas in yellow in Fig. 9), suggesting that the area is a critical region where freshwater processes highly interact with the coastal processes.

The analyses above are based on current climate conditions. However, the future sea level rise is expected to be three to ten times higher than the current rate of sea level rise by the end of the 21st century (Nicholls and Cazenave, 2010). As a result, the dominant control of sea level on saltwater table variation will be intensified in the future, placing more stress on salt-intolerant vegetation.

4.2. Limitations and future work

We acknowledge that some levels of uncertainty still exist due to the lack of sufficient observation of the hydrological processes for model calibration and validation, and uncertainties in datasets and in the model itself. A detailed discussion of the uncertainties can be found in Zhang et al. (2018). Despite the limitations, this study provides guidance for field observations, which, in turn, will facilitate a more accurate, model-based wetland resilience assessment, especially on a regional scale.

Future research should target improving the HR quantification method. For example, soil moisture change and the frequency and duration of flood can potentially be other indicators of wetland resilience. In addition, future research should use the knowledge of hydrologic resilience gained from this study to understand the threshold response of biogeochemical and geomorphological processes to climate variability and climate change. For instance, with the understanding of saltwater table variation, we can investigate the different ecological response of vegetation species, such as saltwater and freshwater marsh, to sea level rise. Additionally, the influences of human activities on wetland hydrological resilience, such as ditching and land conversion (Liu et al., 2018), must be considered as feedbacks between human and natural system exert significant control over ecosystem resilience to environmental change (Gunderson, 2001; Walker et al., 2006).

5. Conclusions

We developed a quantitative method for characterizing wetland hydrologic resilience by introducing comprehensive metrics of coastal hydrologic processes for multi-scale assessments of coastal wetland resilience. Emphasizing the capacity of coastal wetland in storing and releasing water, we used groundwater table, overland flow rate, and saltwater table as indicators of hydrologic resilience in an updated process-based hydrologic model (PIHM-Wetland). We applied the model approach to coastal wetlands in North Carolina, USA, to investigate its hydrologic resilience to climate disturbances from 1995 to 2014, including multiscale variabilities of precipitation, temperature, and sea level rise. To our knowledge, this is the first study investigating hydrologic resilience to climate variability using a process-based numerical model at multiple spatial and temporal scales in an actual ecosystem.

Our analyses confirmed the existence of threshold climate conditions that controlled the hydrological functions of coastal wetlands. Hydrologic resilience presented different characteristics at different temporal scales. The GWT variation could effectively reflect the hydrologic resilience of the coastal wetland to drought at the seasonal, inter-annual, and daily scales. The variation of overland flow under individual rainfall events can be a good indicator of hydrologic resilience to rainfall events. The saltwater table can be a good indicator of hydrologic resilience to sea level rise. The saltwater table is not sensitive to seasonal climate variability and the annual sea level rise is the primary control of the annual variation of the saltwater table.

This study demonstrates the importance of quantifying wetland resilience at the regional scale, accounting for water supply sources and sinks from adjacent landscape components, such as uplands and the ocean, which together control the hydrodynamics of coastal wetland ecosystems. This study also confirmed the necessity of quantifying hydrologic resilience from long time series data analysis, that is more likely to capture threshold responses to the wide range of stochastically varying climate conditions. Although wetlands are very diverse globally, our model-based approach is adaptable to other systems as long as the data required for parameterization are available, providing a consistent framework to assess wetland hydrological resilience to global environmental change.

Acknowledgments

We first thank the constructive comments from the anonymous reviewers. This work was supported by an interagency Carbon Cycle Science award (USDA NIFA 2014-67003-22068). Additional support was provided by the U.S. Forest Service (13-JV-11330110-081) and the Carolinas Integrated Sciences and Assessments program (NOAA 13-2322). Significant in-kind operational support was provided by the U.S. Fish and Wildlife Service, Alligator River National Wildlife Refuge. We would also like to acknowledge the high-performance computing support from Cheyenne provided by NCAR's Computational and Information Systems Laboratory, sponsored by the National Science Foundation.

Appendix A. Supplementary material

Supplementary data to this article can be found online at https://doi.org/10.1016/j.jhydrol.2018.10.048.

References

Ardón, M., Morse, J.L., Colman, B.P., Bernhardt, E.S., 2013. Drought-induced saltwater incursion leads to increased wetland nitrogen export. Global Change Biol. 19 (10), 2976–2985.

Beven, K.J., 2011. Rainfall-Runoff Modelling: The Primer. John Wiley & Sons.

Bruland, G.L., Richardson, C.J., 2006. Comparison of soil organic matter in created, restored and paired natural wetlands in North Carolina. Wetlands Ecol. Manage. 14 (3), 245–251. https://doi.org/10.1007/s11273-005-1116-z.

Burkett, V., Kusler, J., 2000. Climate Change: Potential Impacts and Interactions in Wetlands of the United States. Wiley Online Library.

Cahoon, D.R., Hensel, P.F., Spencer, T., Reed, D.J., McKee, K.L., Saintilan, N., 2006. Coastal wetland vulnerability to relative sea-level rise: wetland elevation trends and process controls. Wetlands Nat. Resour. Manage. 271–292.

Chen, F., Mitchell, K., Schaake, J., Xue, Y., Pan, H.L., Koren, V., Duan, Q.Y., Ek, M., Betts, A., 1996. Modeling of land surface evaporation by four schemes and comparison with FIFE observations. J. Geophys. Res.: Atmos. 101 (D3), 7251–7268.

Conner, W.H., Mihalia, I., Wolfe, J., 2002. Tree community structure and changes from 1987 to 1999 in three Louisiana and three South Carolina forested wetlands. Wetlands 22 (1), 58–70.

Dai, Y., Zeng, X., Dickinson, R.E., Baker, I., Bonan, G.B., Bosilovich, M.G., Denning, A.S., Dirmeyer, P.A., Houser, P.R., Niu, G., 2003. The common land model. Bull. Am. Meteorol. Soc. 84 (8), 1013–1023.
Day, J.W., Christian, R.R., Boesch, D.M., Yáñez-Arancibia, A., Morris, J., Twilley, R.R., Naylor, L., Schaffner, L., 2008. Consequences of climate change on the ecogeomorphology of coastal wetlands. Estuaries Coasts 31 (3), 477–491.
Desantis, L.R., Bhotika, S., Williams, K., Putz, F.E., 2007. Sea-level rise and drought interactions accelerate forest decline on the Gulf Coast of Florida, USA. Global Change Biol 13 (11), 2349–2360.
Dickinson, E., Henderson-Sellers, A., Kennedy, J., 1993. Biosphere-atmosphere transfer scheme (BATS) version 1e as coupled to the NCAR community climate model.
Dickinson, R.E., 1984. Modeling evapotranspiration for three-dimensional global climate models. Climate Process. Climate Sensitivity 58–72.
Fagherazzi, S., Marani, M., Blum, L.K., 2004. The Ecogeomorphology of Tidal Marshes. American Geophysical Union.
Ferguson, G., Gleeson, T., 2012. Vulnerability of coastal aquifers to groundwater use and climate change. Nat. Climate Change 2 (5), 342.
Folke, C., 2006. Resilience: the emergence of a perspective for social–ecological systems analyses. Global Environ. Change 16 (3), 253–267.
Folke, C., Carpenter, S., Elmqvist, T., Gunderson, L., Holling, C.S., Walker, B., 2002. Resilience and sustainable development: building adaptive capacity in a world of transformations. AMBIO: J. Human Environ. 31 (5), 437–440.
Folke, C., Carpenter, S., Walker, B., Scheffer, M., Elmqvist, T., Gunderson, L., Holling, C.S., 2004. Regime shifts, resilience, and biodiversity in ecosystem management. Annu. Rev. Ecol., Evol., System. 35.
Freeze, R.A., 1980. A stochastic-conceptual analysis of rainfall-runoff processes on a hillslope. Water Resour. Res. 16 (2), 391–408.
Fry, J.A., Xian, G., Jin, S., Dewitz, J.A., Homer, C.G., Limin, Y., Barnes, C.A., Herold, N.D., Wickham, J.D., 2011. Completion of the 2006 national land cover database for the conterminous United States. Photogramm. Eng. Remote Sensing 77 (9), 858–864.
Graetz, K.E., 1973. Seacoast plants of the Carolinas.
Gunderson, L.H., 2000. Ecological resilience—in theory and application. Annu. Rev. Ecol. System. 31 (1), 425–439.
Gunderson, L.H., 2001. Panarchy: Understanding Transformations in Human and Natural Systems. Island Press.
Gunderson, L.H., Pritchard, L., 2012. Resilience and the Behavior of Large-Scale Systems. Island Press.
Gupta, A.D., 1985. Approximation of salt-water interface fluctuation in an unconfined coastal aquifer. Ground Water 23 (6), 783–794. https://doi.org/10.1111/j.1745-6584.1985.tb01958.x.
Holling, C.S., 1973. Resilience and stability of ecological systems. Annu. Rev. Ecol. System. 4 (1), 1–23.
Holling, C.S., Gunderson, L.H., 2002. Resilience and adaptive cycles. In: Panarchy: Understanding Transformations in Human and Natural Systems, pp. 25–62.
Kemp, A.C., Horton, B.P., Culver, S.J., 2009. Distribution of modern salt-marsh foraminifera in the Albemarle-Pamlico estuarine system of North Carolina, USA: implications for sea-level research. Mar. Micropaleontol. 72 (3–4), 222–238.
Kirwan, M.L., Megonigal, J.P., 2013. Tidal wetland stability in the face of human impacts and sea-level rise. Nature 504 (7478), 53–60.
Kozlowski, T.T., 2002. Physiological-ecological impacts of flooding on riparian forest ecosystems. Wetlands 22 (3), 550–561.
Kumar, M., 2009. Toward a hydrologic modeling system. Ph.D. thesis. State University, Pennsylvania, pp. 273.
Li, W., Li, L., Fu, R., Deng, Y., Wang, H., 2011. Changes to the North Atlantic subtropical high and its role in the intensification of summer rainfall variability in the southeastern United States. J. Climate 24 (5), 1499–1506.
Liu, X., et al., 2018. Drought and thinning have limited impacts on evapotranspiration in a managed pine plantation on the southeastern United States coastal plain. Agric. For. Meteorol. 262, 14–23. https://doi.org/10.1016/j.agrformet.2018.06.025.
Lu, J., Sun, G., McNulty, S.G., Comerford, N.B., 2009. Sensitivity of pine flatwoods hydrology to climate change and forest management in Florida, USA. Wetlands 29 (3), 826–836.
Lyne, V., Hollick, M., 1979. Stochastic time-variable rainfall-runoff modelling. In: Paper presented at Institute of Engineers Australia National Conference.
McElwee, C., 1985. A model study of salt-water intrusion to a river using the sharp interface approximation. Ground Water 23 (4), 465–475.
Miao, G., Noormets, A., Domec, J.C., Trettin, C.C., McNulty, S.G., Sun, G., King, J.S., 2013. The effect of water table fluctuation on soil respiration in a lower coastal plain forested wetland in the southeastern US. J. Geophys. Res.: Biogeosci. 118 (4), 1748–1762.
Michener, W.K., Blood, E.R., Bildstein, K.L., Brinson, M.M., Gardner, L.R., 1997. Climate change, hurricanes and tropical storms, and rising sea level in coastal wetlands. Ecol. Appl. 7 (3), 770–801.
Mitsch, W.J., Bernal, B., Nahlik, A.M., Mander, Ü., Zhang, L., Anderson, C.J., Jørgensen, S.E., Brix, H., 2013. Wetlands, carbon, and climate change. Landscape Ecol. 28 (4), 583–597.
Montefalcone, M., Parravicini, V., Bianchi, C.N., 2011. Quantification of coastal ecosystem resilience. Treatise Estuarine Coastal Sci. 10, 49–70.
Moorhead, K.K., Brinson, M.M., 1995. Response of wetlands to rising sea level in the lower coastal plain of North Carolina. Ecol. Appl. 5 (1), 261–271.
Nicholls, R.J., 2004. Coastal flooding and wetland loss in the 21st century: changes under the SRES climate and socio-economic scenarios. Global Environ. Change 14 (1), 69–86.
Nicholls, R.J., Cazenave, A., 2010. Sea-level rise and its impact on coastal zones. Science 328 (5985), 1517–1520.
NOAA, 2017. Mean Sea Level Trend of 8652587 Oregon Inlet Marina, North Carolina, edited, NOAA Tide and Currents.
Peterson, T., Western, A., Argent, R., 2012. Analytical methods for ecosystem resilience: a hydrological investigation. Water Resour. Res. 48 (10).
Polo, J.F., Ramis, F.J.R., 1983. Simulation of salt water–fresh water interface motion. Water Resour. Res. 19 (1), 61–68.
Richardson, C.J., 1991. Pocosins: an ecological perspective. Wetlands 11 (1), 335–354.
Richter, B.D., Baumgartner, J.V., Powell, J., Braun, D.P., 1996. A method for assessing hydrologic alteration within ecosystems. Conserv. Biol. 10 (4), 1163–1174.
Ridolfi, L., D'Odorico, P., Laio, F., 2006. Effect of vegetation–water table feedbacks on the stability and resilience of plant ecosystems. Water Resour. Res. 42 (1).
Riggs, S.R., York, L.L., Wehmiller, J.F., Snyder, S.W., 1992. Depositional Patterns Resulting From High Frequency Quaternary Sea Level Fluctuations In Northeastern North Carolina. North Carolina Sea Grant, Raleigh. Pub. no. UNC-SG-03-04, 152.
Rodríguez-Iturbe, I., Porporato, A., 2007. Ecohydrology of Water-Controlled Ecosystems: Soil Moisture and Plant Dynamics. Cambridge University Press.
Sellers, P., Mintz, Y., Sud, Y.E.A., Dalcher, A., 1986. A simple biosphere model (SiB) for use within general circulation models. J. Atmos. Sci. 43 (6), 505–531.
Shamir, U., Dagan, G., 1971. Motion of the seawater interface in coastal aquifers: a numerical solution. Water Resour. Res. 7 (3), 644–657.
Soil Survey Staff, 2016. The Gridded Soil Survey Geographic (gSSURGO) Database for North Carolina, edited by U. S. D. o. Agriculture, United States Department of Agriculture, Natural Resources Conservation Service, https://gdg.sc.egov.usda.gov/.
Thrush, S.F., Hewitt, J.E., Dayton, P.K., Coco, G., Lohrer, A.M., Norkko, A., Norkko, J., Chiantore, M., 2009. Forecasting the limits of resilience: integrating empirical research with theory. Proc. R. Soc. London B: Biol. Sci rspb20090661.
Tufford, D., 2011. Shallow water table response to seasonal and interannual climate variability. T. Asabe 54 (6), 2079–2086.
Walker, B., Gunderson, L., Kinzig, A., Folke, C., Carpenter, S., Schultz, L., 2006. A handful of heuristics and some propositions for understanding resilience in social-ecological systems. Ecol. Soc. 11 (1).
Williams, K., MacDonald, M., Sternberg, L.d.S.L., 2003. Interactions of storm, drought, and sea-level rise on coastal forest: a case study. J. Coastal Res. 1116–1121.
Winter, T.C., 2000. The vulnerability of wetlands to climate change: a hydrologic landscape perspective. JAWRA J. Am. Water Resour. Assoc. 36 (2), 305–311.
Wösten, J., Lilly, A., Nemes, A., Le Bas, C., 1999. Development and use of a database of hydraulic properties of European soils. Geoderma 90 (3), 169–185.
Xia, Y., Mitchell, K., Ek, M., Sheffield, J., Cosgrove, B., Wood, E., Luo, L., Alonge, C., Wei, H., Meng, J., 2012. Continental-scale water and energy flux analysis and validation for the North American Land Data Assimilation System project phase 2 (NLDAS-2): 1. Intercomparison and application of model products. J. Geophys. Res.: Atmos. 117 (D3).
Zhang, Y., Li, W., Sun, G., Miao, G., Noormets, A., Emanuel, R., King, J.S., 2018. Understanding coastal wetland hydrology with a new regional scale process-based hydrologic model. Hydrol. Process. https://doi.org/10.1002/hyp.13247.
Zhang, Y., Slingerland, R., Duffy, C., 2016. Fully-coupled hydrologic processes for modeling landscape evolution. Environ. Modell. Softw. 82, 89–107.
Zhu, J., Sun, G., Li, W., Zhang, Y., Miao, G., Noormets, A., McNulty, S.G., King, J.S., Kumar, M., Wang, X., 2017. Modeling the potential impacts of climate change on the water table level of selected forested wetlands in the southeastern United States. Hydrol. Earth Syst. Sci. 21 (12), 6289–6305. https://doi.org/10.5194/hess-21-6289-2017.